



# Eco-evolutionary dynamics further weakens mutualistic interaction and coexistence under population decline

Avril Weinbach<sup>1,2</sup> · Nicolas Loeuille<sup>1</sup> · Rudolf P. Rohr<sup>2</sup>

Received: 26 January 2022 / Accepted: 18 March 2022  
© The Author(s), under exclusive licence to Springer Nature Switzerland AG 2022

## Abstract

With current environmental changes, evolution can rescue declining populations, but what happens to their interacting species? Mutualistic interactions can help species sustain each other when their environment worsens. However, mutualism is often costly to maintain, and evolution might counter-select it when not profitable enough. We investigate how the evolution of the investment in a mutualistic interaction by a focal species affects the persistence of the system. Specifically, using eco-evolutionary dynamics, we study the evolution of the focal species investment in the mutualistic interaction of a focal species (e.g. plant attractiveness via flower or nectar production for pollinators or carbon exudate for mycorrhizal fungi), and how it is affected by the decline of the partner population with which it is interacting. We assume an allocation trade-off so that investment in the mutualistic interaction reduces the species intrinsic growth rate. First, we investigate how evolution changes species persistence, biomass production, and the intensity of the mutualistic interaction. We show that concave trade-offs allow evolutionary convergence to stable coexistence. We next assume an external disturbance that decreases the partner population by lowering its intrinsic growth rate. Such declines result in the evolution of lower investment of the focal species in the mutualistic interaction, which eventually leads to the extinction of the partner species. With asymmetric mutualism favouring the partner, the evolutionary disappearance of the mutualistic interaction is delayed. Our results suggest that evolution may account for the current collapse of some mutualistic systems like plant-pollinator ones, and that restoration attempts should be enforced early enough to prevent potential negative effects driven by evolution.

**Keywords** Adaptive dynamics · Plant attractiveness · Pollinators decline · Evolutionary murder · Asymmetrical interactions · Alternative stable states

---

✉ Avril Weinbach  
avril.weinbach.pro@gmail.com

<sup>1</sup> Institut of Ecology and Environmental Sciences (iEES-Paris), Sorbonne Université, CNRS, Place Jussieu, 75005 Paris, France

<sup>2</sup> Department of Biology, Ecology and Evolution, University of Fribourg, Fribourg, Switzerland

## Introduction

Facing current global change, evolutionary mechanisms can help maintain biodiversity. Evolutionary rescue (Ferriere and Legendre 2013; Carlson et al. 2014) corresponds to the selection of new traits in population collapsing with environmental changes that allow for a demographic bounce. The signature for evolutionary rescue is the increase in frequency of the allele and corresponding phenotype robust to the new environment, correlatively to the population bounce. While this can be easily highlighted in lab experiments, it has so far been seldom observed in nature. In their review Carlson et al. (2014) cite, for example, a previous study showing the adaptation of some *Chlorella* species, but not all, after strong acidification of many Canadian lakes with industrial pollution.

However, species are not isolated from one another and interaction might interfere with this evolutionary process. Mutualism is an interaction that has already been intensively studied, and proven to be fragile to global changes (Toby Kiers et al. 2010). Echoing to that loss of interactions is that of biodiversity and ecosystem services such as pollination (Willmer 2011a) and seed dispersal (Jordano et al. 2010) and effective carbon and nutrient cycles (Wilson et al. 2009). While several reviews like that of Potts et al. (2010) point out the critical ecological crises we are undergoing, Toby Kiers et al. (2010) add that mutualism, by binding species to a common fate, could create an evolutionary breakdown. With environmental changes, mutualism can become costly to maintain. Aside from co-extinction of the two interacting species, evolution can lead to mutualism loss, partner switch, or even a shift to antagonism. They thoroughly present how the different types of mutualisms are specifically sensitive or resistant to breakdown depending on the global change drivers. For example, plant-pollinator mutualism could be strongly affected by climate change and habitat fragmentation, while plant-rhizosphere mutualisms will be more affected by nutrient enrichment and the introduction of exotic species.

Mutualistic systems, like all other systems of interacting species, will respond differently to global change (Tylianakis et al. 2008). Facing a similar environmental perturbation, some species may show strong population decrease, while their partner species better cope with the environmental change. However, because the fitness of the two partners are positively linked (mutualistic interaction), the fitness decrease of any of the partner species indirectly harms its interactor, reducing its potential for evolutionary rescue and slowing its evolution (evolutionary inertia; Loeuille 2019). For mutualism, and especially obligatory ones, this might lead to species extinction, driven by the evolutionary disinvestment of its interactor. This effect is called an evolutionary murder (name suggested by Parvinen in 2005).

For instance, plants have been shown to evolve rapidly to changing pollinator populations (Darwin 1877; Parmesan 2006; Bodbyl Roels and Kelly 2011; Hopkins and Rausher 2012). A recent study from Gervasi and Schiestl (2017) experimentally shown that changes in pollinator communities affect plant trait evolution after only eleven generations. Exposed to bumblebees, which are very efficient pollinators of *Brassica rapa*, the plants evolved toward more attractive traits to those pollinators (e.g. traits attracting pollinators such as volatile organic compounds, flower size, or plant height). Moreover, hoverflies, which are less efficient pollinators of *B. rapa*, caused a 15-fold increase in self-reproduction and a reduction in plant attractiveness. Given these experimental results, the current change and reshaping of pollinator communities may affect the evolution of plant species, which in turn could influence coexistence with their interacting pollinators, i.e., an eco-evolutionary feedback loop.

Plant-mycorrhizal fungi interactions are another type of mutualism affected by global changes. The mycorrhizal fungi can for example fix inorganic nitrogen and provide this essential nutrient to the plant, who, in exchange, transfers via its roots carbon products to the fungi. Several experiments already shown that enriching the soil in nitrogen (often from anthropogenic sources in natural environments) disturbs this mutualistic exchange, by inducing a shift in the allocation to the mycorrhizal structures (Johnson et al. 2003) and the composition of the mycorrhizal community (Egerton-Warburton et al. 2007). This can in turn affects the plant community, and can even facilitate the invasion of alien plant species (Nijjer et al. 2008).

Theoretical studies have investigated the ecological (Goh 1979; Thébault and Fontaine 2010; Rohr et al. 2014; Saavedra et al. 2016) and evolutionary dynamics (Ferriere et al. 2002; De Mazancourt and Schwartz 2010; Toby Kiers et al. 2010; Georgelin and Loeuille 2016; Valdovinos et al. 2016) of mutualistic communities such as plant-pollinators or plant-fungi. In particular, the evolution of plant selfing with changing pollinator communities has been studied in several papers (Cheptou and Massol 2009; Lepers et al. 2014; Astegiano et al. 2015). Thomann et al. (2013) even suggested that the decrease in pollinator richness and density could intensify pollen limitation. They propose that plants could in turn adapt either by increasing autonomous selfing or reinforcing the interaction with pollinators. Here we study the consequences of a declining population (e.g. pollinator collapse) on the eco-evolutionary dynamics of a two-species mutualistic system (e.g. plant-pollinator or plant-fungi). Specifically, using the adaptive dynamics framework, we study the eco-evolution of the investment in mutualism of a focal species. We assume that the evolving focal species does not rely exclusively on its mutualistic partner (facultative mutualism), while the partner species can either be in an obligatory or in a facultative mutualism. This framework explicitly accounts for the eco-evolutionary feedback loop between the two species. We clarify when evolution leads to high or low investment in mutualism and determine the conditions under which evolution leads to the coexistence of the whole system. We then show that a declining partner population often results in a counter-selection of the investment in mutualism of the focal species, which eventually enhances the population declines. For simplicity in the narrative, in the following, we will use the example of a plant-pollinator system. The adaptive trait is the plant investment, and the declining population is the pollinator. However, our approach remains general and can be applied to other mutualistic systems.

## Plant-pollinator model and ecological dynamics

We consider a simple system with two interacting species; a plant with biomass density  $P$ , and a pollinator with biomass density  $A$ . Note that this model is formulated as a general model of mutualism rather than very specifically tied to plant-pollinator interactions so that results may also concern other mutualistic systems. The community dynamics are given by a Lotka-Volterra type model:

$$\begin{cases} \frac{dA}{dt} = A(r_A - c_A A + \alpha \gamma_P P) \\ \frac{dP}{dt} = P(r_P - c_P P + \alpha \gamma_A A) \end{cases} \quad (1)$$

A schematic view of the system is given in Fig. 1. The parameters  $r_A$  and  $r_P$  correspond to the intrinsic growth rate of the pollinator and plant populations, respectively. We assume  $r_P$  to be strictly positive because of other reproduction means, e.g. vegetative reproduction or autogamy. The intrinsic growth rate of the pollinator ( $r_A$ ) can be positive (in which

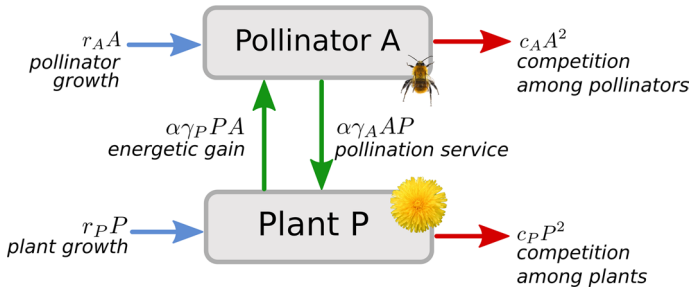
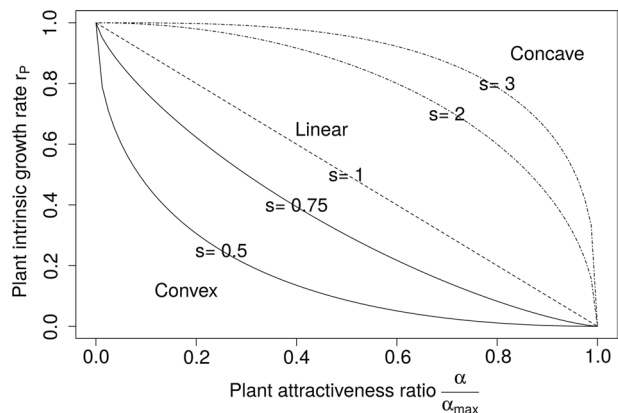


**Fig. 1** Population variation rates of plant  $P$  and pollinator  $A$ . Blue arrows indicate the density variations via other means than the mutualistic interaction, green arrows the effects of the mutualistic interaction, and red arrows the effects of intraspecific competition. Note that the plant intrinsic growth rate  $r_P$  is in trade-off with the plant attractiveness  $\alpha$ . The parameters are described in the main text

case the pollinator has access to alternative resources that allow a positive intrinsic growth rate) or negative (in which case the pollinator strictly needs the plant species, obligatory mutualism). Parameters  $c_A$  and  $c_P$  modulate intraspecific competition for the two species. Mutualistic interactions are given by  $\alpha\gamma_A$  and  $\alpha\gamma_P$ , with  $\gamma_P$  the fitness gain provided by the plant (via nectar, pollen and/or other plant exudates) to the pollinator, and  $\gamma_A$  the fertilisation provided by the pollinator to the plant. Because we consider mutualism as the net benefit obtained by both species, both  $\gamma$  parameter values are assumed positive in our model. We modulate the intensity of the interaction between the two species with the parameter  $\alpha$ . While the interaction depends on biological traits from both interactors (e.g. pollinator morphology or flight capacities, plant attractiveness), we have chosen to model it as a plant-dependent trait and have therefore linked it to other plant traits via a trade-off function (Fig. 2). We interpret it here as the attractiveness of the plant for the pollinator, and it corresponds to the trait that is under selection in the rest of the study. This plant attractiveness includes investment in various characters such as the number of flowers, their shape, their colour, volatile organic compound (VOCs) that attract insects with their odour, plant height, flowering duration or nectar quantity and quality (see part II in Willmer 2011a). Note that in our model, the attractiveness trait we consider has both an intrinsic cost for the plant and has a direct positive effect on the strength of the mutualism. Consequently, we

**Fig. 2** Variation of the attractiveness ratio  $\frac{\alpha}{\alpha_{\max}}$  with the plant intrinsic growth rate  $r_P$  depending on the trade-off strength. Continuous lines show convex trade-offs, the dashed line a linear trade-off, and dashed-dotted lines concave trade-offs



only here model cases of honest signals, and leave out the evolution of cheating associated with these traits.

Extrapolating from previous results (Goh 1979), coexistence is stable provided:

$$\begin{cases} \frac{\alpha\gamma_P r_P + c_P r_A}{c_A c_P - \alpha^2 \gamma_A \gamma_P} > 0 \\ \frac{\alpha\gamma_A r_A + c_A r_P}{c_A c_P - \alpha^2 \gamma_A \gamma_P} > 0 \\ \alpha^2 \gamma_A \gamma_P < c_A c_P \end{cases} \tag{2}$$

The first two inequalities give the condition for the existence of an equilibrium point allowing positive densities (i.e. feasibility conditions). The last inequality ensures the stability of the equilibrium. According to Goh (1976), in the case of two interacting species, conditions for a feasible and locally stable equilibrium with intraspecific interactions regulating the population densities implies its global stability. The globally stable equilibrium is then:

$$\begin{cases} A^* = \frac{\alpha\gamma_P r_P + c_P r_A}{c_A c_P - \alpha^2 \gamma_A \gamma_P} \\ P^* = \frac{\alpha\gamma_A r_A + c_A r_P}{c_A c_P - \alpha^2 \gamma_A \gamma_P} \end{cases} \tag{3}$$

If the stability condition is not fulfilled, i.e., interspecific mutualism is stronger than intraspecific competition, the positive feedback loop resulting from interspecific mutualism may drive the system towards infinite growth. In such cases, other limiting factors (e.g. pathogen, predators, or new competitors) eventually regulate the populations. Since these factors are not taken into account in our model assumptions, we define a maximum plant attractiveness  $\alpha_{cl}$  below which stability is guaranteed:

$$\alpha_{cl} = \sqrt{\frac{c_A c_P}{\gamma_A \gamma_P}}. \tag{4}$$

We allow the evolution of  $\alpha$  between zero (no investment in attractiveness) and this maximal level  $\alpha_{max} < \alpha_{cl}$ . We could also have controlled the infinite growth of our system by choosing a saturating function for the mutualistic interaction. For instance, Holland and DeAngelis (2010) use a saturating (Holling type II) function. The general shape of mutualistic functional responses is however unknown due to the lack of empirical information. Our choice of a linear functional response allows explicit analytical computations and has the advantage to keep the model general and applicable to mutualistic interactions other than pollination, i.e. ant-plant, plant-rhizosphere or coral-zooxanthellae mutualisms (Toby Kiers et al. 2010).

### Evolution of plant attractiveness

We study the evolution of plant attractiveness ( $\alpha$ ), assuming an allocation trade-off affecting the plant intrinsic growth rate  $r_P$  (Willmer 2011b). Its biomass can grow either via a reproduction process dependent on the interaction with its mutualist (e.g. pollination) whose intensity is controlled by its attractiveness  $\alpha$ , or via intrinsic growth (e.g. vegetative growth) and self-reproduction. The plant has a given quantity of energy that is divided

between these two growth modes (Obeso 2002; Willmer 2011b), so that we assume  $r_p$  to be a decreasing function of the attractiveness  $\alpha$ :

$$\left(\frac{r_p}{r_{pmax}}\right)^s + \left(\frac{\alpha}{\alpha_{max}}\right)^s = 1. \tag{5}$$

The plant maximal intrinsic growth rate  $r_{pmax}$  can, by rescaling time unit and without loss of generality, be fixed to one. It can then be expressed as function of its attractiveness as:

$$r_p(\alpha) = \left(1 - \left(\frac{\alpha}{\alpha_{max}}\right)^s\right)^{1/s}. \tag{6}$$

The  $s$  exponent controls the trade-off shape. When  $s = 1$  there is a linear relationship between  $r_p$  and  $\alpha$ . When  $0 < s < 1$  the trade-off is convex. On the opposite,  $s > 1$  produces a concave trade-off (as shown in Fig. 2).

We follow the evolution of plant attractiveness using adaptive dynamics techniques (Dieckmann and Law 1996; Geritz et al. 1998). Under adaptive dynamics hypotheses (see supplementary material section A for a full description of the method and hypotheses) we can model the evolution of plant attractiveness and its consequences on species density dynamics, and the feedback of species density on the evolutionary process (Dieckmann and Law 1996). Evolution then proceeds by the successive invasions and replacements of resident by mutant populations. Such dynamics are approximated, given rare and small mutations, by the canonical equation (Dieckmann and Law 1996):

$$\frac{d\alpha}{dt} = \frac{1}{2}\mu\sigma^2P^*(\alpha)\left.\frac{\partial\omega(\alpha_m, \alpha)}{\partial\alpha_m}\right|_{\alpha_m\rightarrow\alpha}. \tag{7}$$

The term  $\frac{1}{2}\mu\sigma^2P(\alpha)$  encapsulates the phenotypic variability brought by the mutation process on which selection can act ( $\mu$  is the probability of mutation per birth and  $\sigma^2$  the variance of variance of mutational steps; see Dieckmann and Law 1996). The function  $\omega(\alpha_m, \alpha)$  is the relative fitness of a rare mutant of trait  $\alpha_m$  in a resident population of trait  $\alpha$ . Its partial derivative, the last term of Eq. (7) defines the selection gradient. It gives the direction of evolution; a positive gradient selects larger attractiveness, while a negative gradient selects smaller trait values. The relative fitness of the mutant is computed as the *per capita* growth rate of a rare mutant population in a resident population at ecological equilibrium (3):

$$\omega(\alpha_m, \alpha) = \frac{1}{P_m}\left.\frac{dP_m}{dt}\right|_{P_m\rightarrow 0} = r_p(\alpha_m) - c_pP^*(\alpha) + \alpha_m\gamma_A A^*(\alpha), \tag{8}$$

Eco-evolutionary equilibrium (called a singular strategy) occurs when the phenotypic trait stops varying, i.e. Equation 7 equals 0. Since its first part is always positive, it corresponds to  $\hat{\alpha}$  values for which the selection gradient is null:

$$\left.\frac{\partial\omega(\alpha_m, \alpha)}{\partial\alpha_m}\right|_{\alpha_m\rightarrow\hat{\alpha}} = \frac{dr_p(\hat{\alpha})}{d\hat{\alpha}} + \gamma_A A^*(\hat{\alpha}) = 0. \tag{9}$$

At singularities, costs in terms of energy dedicated to alternative means of reproduction ( $dr_p(\hat{\alpha})/d\hat{\alpha}$ ) therefore match pollination benefits ( $\gamma_A A^*(\hat{\alpha})$ ). The existence of a singular strategy is not enough to guarantee that evolutionary dynamics locally lead to it (convergence condition) or that it persists (non-invasibility condition, i.e. resistance to invasion by nearby mutants). A singular strategy that is both convergent and non-invasive is called a continuously stable strategy (CSS) (Christiansen 1991). Evolution toward a CSS guarantees the coexistence of the two species. This and other singularity types are presented in Fig. 3. Calculation of the second and cross-derivative of the fitness function determines criteria for convergence and invasibility (Marrow et al. 1996). The mathematical computation for the existence of singular strategies and their convergence and invasibility properties are detailed in the supplementary material sections A and B.

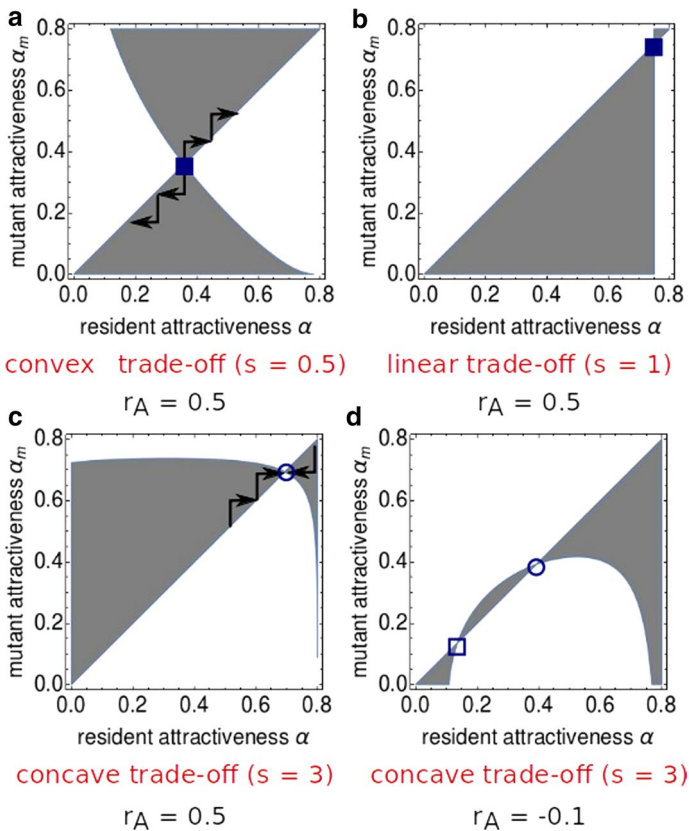


**Fig. 3** Pairwise invasibility plots (PIPs) representing the invasibility potential of a rare mutant within a resident plant population at ecological equilibrium. Grey areas indicate that the mutant relative fitness  $\omega(\alpha_m, \alpha)$  is positive, so that it invades and replaces the resident population. In panels **a** and **c**, arrows show the direction of evolutionary trajectories. The system exhibits several singular strategies depending on the parameter values. Circles represent convergent strategies, whereas squares are non-convergent. Filled symbols represent invulnerable strategy, while not filled symbols are non-invasive. In panels **a** and **b**, the singular strategy is non-convergent and invulnerable (repellor). In panel **c**, the singular strategy is convergent and non-invasive (CSS). Panel **d** displays two strategies, one CSS and one which is non-convergent and non-invasive (Garden of Eden). Parameter values are:  $c_A = c_p = \gamma_A = \gamma_p = 1$ , and  $\alpha_{max} = 0.8 * \alpha_{cl}$

Equation (9) can be solved analytically for particular sets of parameters (e.g. in the linear case when  $s = 1$ , see supplementary material section A). For other cases, we graphically determine convergence and invasibility using pairwise invasibility plots (Fig. 3). It is possible to show (supplementary material section B), as illustrated in Fig. 3, that among the particular trade-offs that we study (Eq. 6), only concave allocation trade-offs lead to non-invasible strategies. Therefore, CSSs, being non-invasible, are only obtained with a concave trade-off function. Convergence depends on the pollinator's intrinsic growth rate (Fig. 3c and d). Mathematical analyses show that linear trade-offs lead to singular strategies that are not convergent (supplementary material section B). In that specific case, we can express explicitly the formula of the attractiveness at eco-evolutionary equilibrium (Equation (A7) in supplementary material section A). We observe the evolution of plant higher attractiveness when the plant mutualistic benefit decreases ( $\gamma_P$ ) or when intraspecific competition increase ( $c_P$  and  $c_A$ ). For non-linear trade-offs, convergence criteria cannot be solved and we rely on numerical investigations and pairwise invasibility plots (PIP). A PIP plot shows in grey, for a given resident trait on the  $x$ -axis, the set of mutant traits,  $y$ -axis, that can invade it. Evolutionary singularities occur at the intersection of the diagonal and of the zero-fitness contour. Whether these strategies are convergent or divergent, invulnerable or non-invasible can be deduced directly from the plot (Geritz et al. 1998).

For positive pollinator intrinsic growth rate, given concave trade-offs, we obtain only one convergent stable singular strategy (CSS) at which ecological coexistence is granted. For negative pollinator intrinsic growth rate, the system exhibits a second singular strategy that is a Garden of Eden (non-convergent and non-invasible), i.e. a stable strategy that can never be reached by nearby mutants. While the conditions of existence of multiple singularities cannot be completely mathematically derived, our results suggest that it occurs for very concave trade-offs. The case where pollinator growth rate entirely relies on the mutualistic interaction ( $r_A = 0$ ) can for instance be analysed mathematically and reveals that two singularities will emerge when  $s \geq 2$  (supplementary material section C).

For convex trade-offs (Fig. 3a and b), we always observe repellers (non-convergent and invulnerable). Starting above the repeller, attractiveness increases to reach the maximum value ( $\alpha = \alpha_{max}$ ) and the plant growth relies only on the mutualistic interaction. In that case plant pollination can only be maintained if pollinators are present and with a positive intrinsic growth rate (obligatory mutualism on the plant side). Starting below the repeller, attractiveness evolves to zero, so that the two species no longer interact at the end of the evolutionary dynamics (e.g. complete selfing or clonal reproduction). As there is no more interaction it is trivial that pollinators are maintained only if their intrinsic growth rate is positive. In the following, because we are interested in the species long-term coexistence with intermediate investment in the mutualistic interaction (i.e., CSS singularities), we only study concave trade-off functions (i.e.  $s > 1$ ).

## Consequences of pollinator population decline

Now that we have characterised the eco-evolutionary dynamics of the plant-pollinator system, we study how pollinator decline may affect its outcome. We simulate less favourable environmental conditions for pollinators (e.g. habitat fragmentation, pesticides, diseases) by decreasing their intrinsic growth rate ( $r_A$ ). We illustrate the effects of this disturbance through Ecology-Evolution-Environment ( $E^3$ ) diagrams (Dieckmann and Ferrière 2004; Ferrière and Legendre 2013). These diagrams, presented in Figs. 4 and 5, show the



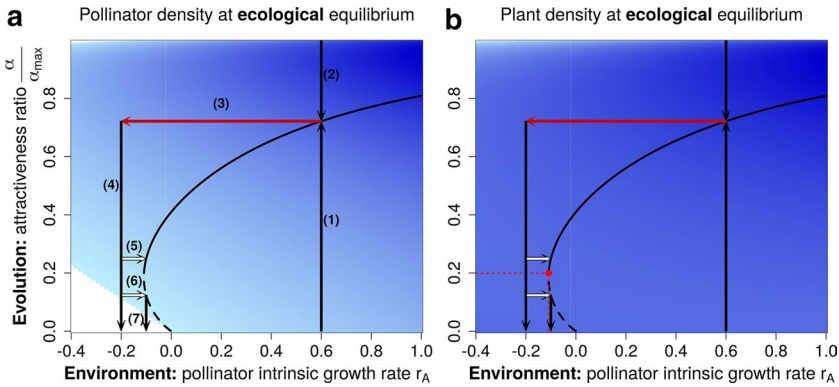


**Fig. 4** Ecology–evolution–environment ( $E^3$ ) diagram representing the impact of pollinator environmental deterioration on the evolution of plant attractiveness and on pollinator (panel **a**) and plant (panel **b**) equilibrium biomass densities. White areas show parameters for which extinction occurs for either plants or pollinators. The blue intensity correlates with population densities of pollinators (panel **a**) or plants (panel **b**). Black lines show the position of singular strategies; continuous lines show convergent and non-invasible singular strategies (CSS), and dashed lines show Garden of Edens (non-invasible, divergent). Vertical black arrows (1, 2, 4, 7) display the direction of evolution. Environmental disturbance is represented by a red arrow (3). White arrows (5, 6) represent restoration attempts at different times along the evolutionary trajectory. On panel **b**) the red point and dotted lines represent the lowest  $r_A$  and  $\frac{\alpha}{\alpha_{max}}$  values for allowing a CSS, therefore the maintenance of the mutualistic interaction. This point is what we call an eco-evolutionary tipping point. Parameters values are  $s = 2.5, c_A = c_P = \gamma_P = 1, \gamma_A = 0.2$ , and  $\alpha_{max} = 0.8 * \alpha_{cl}$ . Similar  $E^3$  diagrams can be found in Dieckmann and Ferrière 2004; Ferrière and Legendre 2013

outcome of eco-evolutionary dynamics as a function of the environmental parameter, here the pollinator intrinsic growth rate  $r_A$ . Figure 4 exhibits two types of singular strategies depending on the pollinator intrinsic growth rate.

For positive pollinator intrinsic growth rates ( $r_A > 0$ ), i.e. in “good pollinator environments”, we observe a convergent and stable singular strategy (CSS, continuous line). Any ecological system with positive  $r_A$  evolutionarily converges toward intermediate attractiveness  $\alpha$  (arrows (1) and (2) in Fig. 4a).

For negative pollinator intrinsic growth rate  $r_A < 0$ , i.e. in “bad pollinator environments”, we also find a non-convergent strategy, a Garden of Eden (GOE, dashed line). In this case, the system exhibits alternative evolutionary stable states. When plant attractiveness is above the Garden of Eden value, evolution converges toward the CSS, while when below the GOE value, selection leads to ever-decreasing attractiveness that eventually leads to the disappearance of the mutualistic interaction.

If we consider environmental degradation, i.e. a strong decrease of  $r_A$  (red arrow (3) in Fig. 4a), in the absence of evolution, both plant and pollinator populations have positive biomass densities at ecological equilibrium (blue backgrounds on Fig. 4a and b). However, considering evolution, plant attractiveness is counter selected as pollinators are too rare to compensate for the intrinsic costs of attractiveness. Eventually, evolution drives pollinator populations to extinction; an evolutionary murder depicted by arrow (4) in Fig. 4a. Faced with the crash of pollinator populations, restoration attempts may be undertaken (i.e. an increase in  $r_A$  value, e.g. by suppressing pesticides or adding other plant resources for pollinators). Early intervention, depicted by arrow (5), can restore a stable mutualistic interaction. Delayed restoration attempts (white arrow (6)), do not allow such a rescue, as evolutionary trajectories will counteract their effects and lead to the extinction of the pollinator

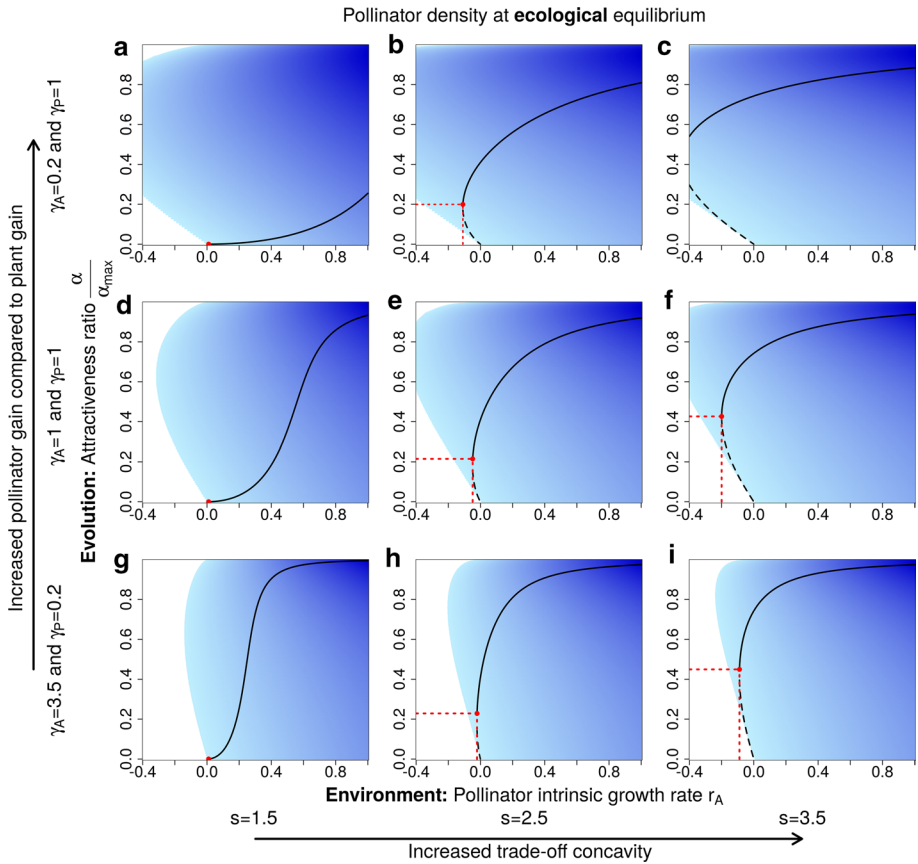


**Fig. 5** Influence of trade-off shape and mutualistic gains on eco-evolutionary dynamics. Columns differ in trade-off concavity. Lines differ in the asymmetry of mutualistic gains: in the top line (panels **a**, **b**, and **c**) pollinators benefit more than plants; the middle line (panels **d**, **e**, and **f**) shows equal gains while in the bottom line plant gains are larger (panels **g**, **h**, and **i**). Red point and dotted lines represent the lowest  $r_A$  and  $\frac{\alpha}{\alpha_{max}}$  values for allowing a CSS and the maintenance of the mutualistic interaction. Colours and lines are the same as in Fig. 4. The parameter values are  $c_A = c_P = 1$  and  $\alpha_{max} = 0.8 * \alpha_{cl}$

(arrow (7)). Note that here we separate timescales for simplicity, and consider that deterioration and restoration are fast compared to the evolutionary dynamics, hence horizontal arrows for these environmental changes.

Finally, we study how trade-off shapes and asymmetry of mutualistic gains affect the eco-evolutionary outcome (Fig. 5). With increasing concavity, the minimum value of pollinator intrinsic growth rate  $r_A$  that allows for a CSS decreases (red dots on Fig. 5), increasing the coexistence domain (i.e. interval of  $r_A$  values that allows species coexistence at an intermediate interaction level). More concave trade-offs therefore allow a larger coexistence domain up to negative values of  $r_A$  (Fig. 5b, c, e, f, h, i). For less concave trade-offs,  $s < 2$ , only a positive pollinator intrinsic growth rate  $r_A$  allows coexistence (Fig. 5a, d, g). Negative pollinator intrinsic growth rates lead to small benefits for the plant, so that attractiveness is counter selected, eventually leading to the pollinator extinction. For stronger concave trade-offs,  $s > 2$ , (Fig. 5b, c, e, f, h, i) we observe qualitatively the same dynamics

as in Fig. 4. For those trade-offs, asymmetric mutualistic gains favouring pollinators allow a larger range of disturbance, including negative intrinsic growth rates  $r_A$ , before attractiveness is counterselected and extinction occurs. Therefore, an increased mutualistic gain of the pollinator relative to that of the plant facilitates the long-term coexistence of the plant-pollinator system. This produces a more robust system that eases a potential restoration process. Note, however, that favouring pollinators' gain over plants leads to lower selected levels of attractiveness (compare Fig. 5 a, b, c vs g, h, i). The same figure but with the plant density at ecological equilibrium can be found in the supplementary material section D. Apart from very high values of investment in attractiveness with strongly negative pollinator growth rates, plant density is always positive.

## Discussion

While from a one species perspective, evolution can help to avoid extinction by fostering adaptation and restoring positive growth rates (evolutionary rescue), we here show an example in which accounting for mutualistic interactions largely modifies this optimistic view. Here, the evolution of one species in response to disturbances acting on its mutualistic interactor selects a further decrease in the interactor population, eventually leading to the demise of the mutualistic interaction. This shows that evolution within mutualistic systems can actually be detrimental to the system's persistence and could undermine restoration attempts. Because we have used a general model of mutualism, this mechanism may concern various systems. This clearly suggests that when investigating the impact of global changes, we need to account for eco-evolutionary dynamics of the species and their interactors.

The model we use is deliberately simple to allow a more complete mathematical study of eco-evolutionary dynamics and to highlight the role of key parameters (e.g. trade-off shapes or mutualistic gains). However, it may be linked to other models that study various types of mutualism. For instance, considering pollination systems and plant reproduction, in line with the presentation of the results, our model recalls previous theoretical works on plant evolution that detail further the reproductive implications (e.g. Cheptou and Massol 2009; Lepers et al. 2014; Astegiano et al. 2015). For instance, Lepers et al. (2014) explicitly modelled the evolution of a plant reproduction system by taking prior selfing and inbreeding depression into account. In particular, they showed that evolution toward high prior selfing (for us of lesser attractiveness) leads first to pollinator extinction (our evolutionary murder). Because they also model the cost resulting from the inbreeding depression, they show that this evolutionary murder may further lead to the extinction of the plant population. However, the model we propose may also be adapted to consider other mutualistic systems. For instance, in plant-mycorrhizae interactions, a resource exchange takes place, where plants provide carbon-based resources (e.g. sugars) to mycorrhizae while they get nutrients from the interaction. Such a situation does fit our hypotheses. The trait  $\alpha$  would then be the quantity of resources provided by the plant (i.e., its investment in the mutualistic interaction), and this production diverts resources from growth and reproduction, therefore fitting our trade-off hypotheses. As such, our model recalls the results of a study by De Mazancourt and Schwartz (2010). They show that mutualism can arise and be evolutionarily selected from a two-species competing model by including trading. Each species can trade the resource it extracts in excess with the other. In our system, this trading would correspond to the benefit  $\alpha\gamma$  provided by the mutualistic interaction. Depending

on the resource availability (the intrinsic growth in our model) the plant can either perform better on its own (possibly at the detriment of the fungi, as in our model) or can benefit from the mutualistic association with a mycorrhizal fungus. The mutualistic trading interaction can extend the coexistence boundaries, i.e. the resource space the two species can live in.

We are aware that the linear Lotka-Volterra structure of our model and the adaptive dynamics methods impose specific working hypotheses that can constrain the applicability of our model (e.g. ecological equilibrium between small mutation steps, asexual reproduction, panmixia). Our model is a better fit for specific reproduction types like that of geitonogamous species. Models that put into equations specific types of mutualistic interactions can better explicit the different biological processes at stake and have a more realistic view of the mechanisms, e.g. Fishman and Hadany pollination model (2010). They show that a complex and biologically detailed resource trade mutualism can be approximated by a Beddington–DeAngelis formula for trophic interactions. However, the previously cited more complex models (Cheptou and Massol 2009; De Mazancourt and Schwartz 2010; Lepers et al. 2014; Astegiano et al. 2015) find a disinvestment in mutualism with declining efficiency similar to the one observed in our simple and more general model, coherent with the results from the experimental evolution studies (Bodbyl Roels and Kelly 2011; Gervasi and Schiestl 2017). They can better detail the potential consequences of this disinvestment on the interactors for a specific mutualistic type.

Our results also highlight that mutualistic interactions could be more or less vulnerable to environmental changes and population declines. For instance, here, only concave allocation trade-offs between plant intrinsic growth rate and investment in mutualism lead to the maintenance of the mutualistic interaction. These trade-offs favour intermediate investments in the mutualistic interaction, while in the case of convex trade-offs, either complete investment or no investment is eventually selected, depending on initial conditions. We kept our study general because trade-off shapes are extremely difficult to measure *in vivo*, and can vary deeply depending on the environment or the species types (Reekie and Bazaz 2011).

Bistability and critical transitions have been highlighted in a variety of ecological situations (e.g. Dercole et al. 2002; Scheffer and Carpenter 2003 in mutualistic system), and result from a strong positive feedback loop. Here we have a similar phenomenon but on an eco-evolutionary scale. If the evolved investment in mutualism before environmental deterioration is above a certain threshold, evolution reinforces the interaction, by increasing the attractiveness values, eventually leading to a stable, coexisting system. On an ecological scale, this interaction reinforcement increases the abundance of both species, which in turn favours the evolution of the focal species investment toward higher value. Below a critical level of evolved investment, the population of the mutualistic partner species is low. Evolution then further decreases investment in mutualism, eventually leading to complete disinvestment in the mutualistic interaction. This runaway selection for decreased investment leads in our case to the evolutionary murder of the partner population by the evolving species (Dieckmann et al. 1995). Note that the trade-off shape modulates the strength of the positive feedback loop. More concave trade-offs decrease the threshold value above which interaction is maintained, thereby facilitating the persistence of the system. Such dynamics have important implications. For instance, consider pollination as the mutualistic interaction. Current data suggest large decreases in pollinator abundances (Biesmeijer et al. 2006). Such pollinator declines are often considered to be directly linked to environmental changes (e.g. habitat change, pesticides in Potts et al. 2010). However, our results suggest that evolutionary components may also be present. If these declines favour plant strategies

that offer less resources, plant evolution may enhance the observed declines. In line with these predictions, empirical observations suggest a decline of flower resources parallel to the pollinator decline (Biesmeijer et al. 2006).

On a management side, alternative stable states and critical transitions have large implications, as systems may then shift abruptly, and large restorations are needed to recover previous states (Scheffer and Carpenter 2003). The eco-evolutionary alternative stable states we describe here have similar implications. Restoration can either be a reduction of the mortality causes of the declining species (banning pesticide, ploughing controlling pests and predators) or the increase in their alternative resource source (plant sowing or nutrient addition). Here we consider that restorations are faster than evolutionary timescales. Evolution can, however, act fast (Gervasi and Schiestl 2017), while restoration timescales largely vary from a few months (e.g. sowing high reward plants) to much longer timescales. Changes in pesticide regulations and applying these regulations may require national or international consensus. Similarly, while a change in the agricultural mode does occur (e.g. from intensive to agroecology), its dynamics happen over decades, while the evolution of plant rewards may happen in just a few generations (Gervasi and Schiestl 2017). Note that, were we to consider longer restoration attempts, we would still observe eco-evolutionary tipping points in our system. Such tipping points also make restoration attempts more difficult from two different points of view. First, the timing of the attempt becomes important. Restoration is only successful when achieved before the threshold attractiveness is evolved. Second, if the system becomes degraded, a small restoration attempt may not be sufficient to recover large populations, but large efforts will have to be undertaken.

While in the face of current changes in the environment, evolution can play a key role in restoring populations and maintaining diversity, our results suggest that in the case of mutualistic interactions, evolution may also favour strategies that eventually further threaten species coexistence. As such, our model echoes recent analyses that highlight the evolutionary fragility of mutualisms, given current changes (Toby Kiers et al. 2010; Loeuille 2019). Because our model is deliberately simple, restricted in its number of interaction types and species, we expect evolutionary effects in complex ecological networks to be more complex and context-dependent. However, we expect that accounting for these covariations of evolutionary dynamics and changes in ecological interactions will be important, and that the effects of evolution will then not systematically be positive.

**Supplementary Information** The online version contains supplementary material available at <https://doi.org/10.1007/s10682-022-10176-7>.

**Acknowledgements** Nicolas Loeuille and Avril Weinbach would like to acknowledge the French National Research Agency (ANR) for funding, as well as the École Normale Supérieure de Lyon. Rudolf P. Rohr acknowledges funding from the Swiss National Science Foundation. Authors would also like to thank Sylvain Billiard and two anonymous reviewers for insightful comments on the present manuscript via the Peer Community In (PCI) reviewing process. The version 5 recommended can be found online on bioRxiv (<https://doi.org/10.1101/570580>) and the recommendation on the Peer Community in Ecology website (<https://doi.org/10.24072/pci.ecology.100089>).

**Authors' contributions** Nicolas Loeuille and Rudolf P. Rohr designed the model. Avril Weinbach performed the analysis with Rudolf P. Rohr. All authors contributed to writing the article, while the first draft was written by Avril Weinbach.

**Funding** Nicolas Loeuille and Avril Weinbach were supported by the French National Research Agency (ANR) through project ARSENIC (grant no. 14-CE02-0012). Avril Weinbach was additionally supported by a doctoral scholarship from the École Normale Supérieure de Lyon. Rudolf P. Rohr acknowledges funding from the Swiss National Science Foundation, Project grant no. 31003A\_182386.

**Availability of data and materials** Not applicable.

**Code availability** The scripts used to produce the data and Figs. 2, 4, 5 and figure C1 and D1 of the supplementary materials can be found in Zenodo (<https://doi.org/10.5281/zenodo.5552426>).

## Declarations

**Conflict of interest** The authors of this manuscript declare that they have no financial conflict of interest with the content of this article.

**Ethics approval** Not applicable.

**Consent to participate** Not applicable.

**Consent for publication** Not applicable.

## References

- Astegiano J, Massol F, Vidal MM, Cheptou P-O Jr, Guimarães PR (2015) The robustness of plant-pollinator assemblages: linking plant interaction patterns and sensitivity to pollinator loss. *PLoS ONE* 10:e0117243. <https://doi.org/10.1371/journal.pone.0117243>
- Biesmeijer JC, Roberts SPM, Reemer M, Ohlemüller R, Edwards M, Peeters T, Schaffers AP, Potts SG, Kleukers R, Thomas CD, Settele J, Kunin WE (2006) Parallel declines in pollinators and insect-pollinated plants in Britain and the Netherlands. *Science* 313:351–354. <https://doi.org/10.1126/science.1127863>
- Bodbyl Roels SA, Kelly JK (2011) Rapid evolution caused by pollinator loss in *Mimulus* *Guttatus*. *Evolution* 65:2541–2552. <https://doi.org/10.1111/j.1558-5646.2011.01326.x>
- Carlson SM, Cunningham CJ, Westley PAH (2014) Evolutionary rescue in a changing world. *Trends Ecol Evol* 29:521–530. <https://doi.org/10.1016/j.tree.2014.06.005>
- Cheptou P, Massol F (2009) Pollination fluctuations drive evolutionary syndromes linking dispersal and mating system. *Am Nat* 174:46–55. <https://doi.org/10.1086/599303>
- Christiansen FB (1991) On Conditions for evolutionary stability for a continuously varying character. *Am Nat* 138:37–50
- Darwin C (1877) On the various contrivances by which British and foreign orchids are fertilised by insects, and on the good effects of intercrossing. John Murray, London.
- De Mazancourt C, Schwartz MW (2010) A resource ratio theory of cooperation. *Ecol Lett* 13:349–359. <https://doi.org/10.1111/j.1461-0248.2009.01431.x>
- Dercole F, Ferriere R, Rinaldi S (2002) Ecological bistability and evolutionary reversals under asymmetrical competition. *Evolution* 56:1081–1090. <https://doi.org/10.1111/j.0014-3820.2002.tb01422.x>
- Dieckmann U, Ferrière R (2004) Adaptive dynamics and evolving biodiversity. *Evolutionary conservation biology*. Cambridge University Press, Cambridge, pp 188–224
- Dieckmann U, Law R (1996) The dynamical theory of coevolution: a derivation from stochastic ecological processes. *J Math Biol* 34:579–612. <https://doi.org/10.1007/BF02409751>
- Dieckmann U, Marrow P, Law R (1995) Evolutionary cycling in predator-prey interactions: population dynamics and the red queen. *J Theor Biol* 176:91–102. <https://doi.org/10.1006/jtbi.1995.0179>
- Egerton-Warburton LM, Johnson NC, Allen EB (2007) Mycorrhizal community dynamics following nitrogen fertilization: a cross-site test in five grasslands. *Ecol Monogr* 77:527–544. <https://doi.org/10.1890/06-1772.1>
- Ferriere R, Legendre S (2013) Eco-evolutionary feedbacks, adaptive dynamics and evolutionary rescue theory. *Phil Trans R Soc B* 368:20120081. <https://doi.org/10.1098/rstb.2012.0081>
- Ferriere R, Bronstein JL, Rinaldi S, Law R, Gauduchon M (2002) Cheating and the evolutionary stability of mutualisms. *Proc R Soc Lond B Biol Sci* 269:773–780. <https://doi.org/10.1098/rspb.2001.1900>
- Fishman MA, Hadany L (2010) Plant–pollinator population dynamics. *Theor Popul Biol* 78:270–277. <https://doi.org/10.1016/j.tpb.2010.08.002>
- Georgelin E, Loeuille N (2016) Evolutionary response of plant interaction traits to nutrient enrichment modifies the assembly and structure of antagonistic-mutualistic communities. *J Ecol* 104:193–205. <https://doi.org/10.1111/1365-2745.12485>
- Geritz SAH, Kisdi E, Mesze G, Metz JAJ (1998) Evolutionarily singular strategies and the adaptive growth and branching of the evolutionary tree. *Evol Ecol* 12:35–57. <https://doi.org/10.1023/A:1006554906681>



- Gervasi DDL, Schiestl FP (2017) Real-time divergent evolution in plants driven by pollinators. *Nat Commun* 8:14691. <https://doi.org/10.1038/ncomms14691>
- Goh BS (1976) Global stability in two species interactions. *J Math Biol* 3:313–318. <https://doi.org/10.1007/BF00275063>
- Goh BS (1979) Stability in models of mutualism. *Am Nat* 113:261–275
- Holland JN, DeAngelis DL (2010) A consumer–resource approach to the density-dependent population dynamics of mutualism. *Ecology* 91:1286–1295. <https://doi.org/10.1890/09-1163.1>
- Hopkins R, Rausher MD (2012) Pollinator-mediated selection on flower color allele drives reinforcement. *Science* 335:1090–1092. <https://doi.org/10.1126/science.1215198>
- Johnson NC, Rowland DL, Corkidi L, Egerton-Warburton LM, Allen EB (2003) Nitrogen enrichment alters mycorrhizal allocation at five mesic to semiarid grasslands. *Ecology* 84:1895–1908. [https://doi.org/10.1890/0012-9658\(2003\)084\[1895:NEAMAA\]2.0.CO;2](https://doi.org/10.1890/0012-9658(2003)084[1895:NEAMAA]2.0.CO;2)
- Jordano P, Forget P-M, Lambert JE, Böhning-Gaese K, Traveset A, Wright SJ (2010) Frugivores and seed dispersal: mechanisms and consequences for biodiversity of a key ecological interaction. *Biol Lett* rsbl20100986. <https://doi.org/10.1098/rsbl.2010.0986>
- Lepers C, Dufay M, Billiard S (2014) How does pollination mutualism affect the evolution of prior self-fertilization? A model. *Evolution* 68:3581–3598. <https://doi.org/10.1111/evo.12533>
- Loeuille N (2019) Eco-evolutionary dynamics in a disturbed world: implications for the maintenance of ecological networks. *F1000Research* 8. <https://doi.org/10.12688/f1000research.15629.1>
- Marrow P, Dieckmann U, Law R (1996) Evolutionary dynamics of predator-prey systems: an ecological perspective. *J Math Biol* 34:556–578. <https://doi.org/10.1007/BF02409750>
- Nijjer S, Rogers WE, Lee C-TA, Siemann E (2008) The effects of soil biota and fertilization on the success of *Sapium sebiferum*. *Appl Soil Ecol* 38:1–11. <https://doi.org/10.1016/j.apsoil.2007.08.002>
- Obeso JR (2002) The costs of reproduction in plants. *New Phytol* 155:321–348. <https://doi.org/10.1046/j.1469-8137.2002.00477.x>
- Parmesan C (2006) Ecological and evolutionary responses to recent climate change. *Annu Rev Ecol Evol Syst* 37:637–669. <https://doi.org/10.1146/annurev.ecolsys.37.091305.110100>
- Parvinen K (2005) Evolutionary suicide. *Acta Biotheor* 53:241–264. <https://doi.org/10.1007/s10441-005-2531-5>
- Potts SG, Biesmeijer JC, Kremen C, Neumann P, Schweiger O, Kunin WE (2010) Global pollinator declines: trends, impacts and drivers. *Trends Ecol Evol* 25:345–353. <https://doi.org/10.1016/j.tree.2010.01.007>
- Reekie E, Bazzaz FA (2011) Reproductive allocation in plants. Elsevier
- Rohr RP, Saavedra S, Bascompte J (2014) On the structural stability of mutualistic systems. *Science* 345:1253497. <https://doi.org/10.1126/science.1253497>
- Saavedra S, Rohr RP, Olesen JM, Bascompte J (2016) Nested species interactions promote feasibility over stability during the assembly of a pollinator community. *Ecol Evol* 6:997–1007. <https://doi.org/10.1002/ece3.1930>
- Scheffer M, Carpenter SR (2003) Catastrophic regime shifts in ecosystems: linking theory to observation. *Trends Ecol Evol* 18:648–656. <https://doi.org/10.1016/j.tree.2003.09.002>
- Thébault E, Fontaine C (2010) Stability of ecological communities and the architecture of mutualistic and trophic networks. *Science* 329:853–856. <https://doi.org/10.1126/science.1188321>
- Thomann M, Imbert E, Devaux C, Cheptou P-O (2013) Flowering plants under global pollinator decline. *Trends Plant Sci* 18:353–359. <https://doi.org/10.1016/j.tplants.2013.04.002>
- Toby Kiers E, Palmer TM, Ives AR, Bruno JF, Bronstein JL (2010) Mutualisms in a changing world: an evolutionary perspective. *Ecol Lett* 13:1459–1474. <https://doi.org/10.1111/j.1461-0248.2010.01538.x>
- Tylianakis JM, Didham RK, Bascompte J, Wardle DA (2008) Global change and species interactions in terrestrial ecosystems. *Ecol Lett* 11:1351–1363. <https://doi.org/10.1111/j.1461-0248.2008.01250.x>
- Valdovinos FS, Brosi BJ, Briggs HM, Moisset de Espanés P, Ramos-Jiliberto R, Martínez ND (2016) Niche partitioning due to adaptive foraging reverses effects of nestedness and connectance on pollination network stability. *Ecol Lett* 19:1277–1286. <https://doi.org/10.1111/ele.12664>
- Willmer P (2011a) *Pollination and Floral Ecology*. Princeton University Press
- Willmer P (2011b) Rewards and costs: the environmental economics of pollination. In: *Pollination and Floral Ecology*. Princeton University Press, pp 234–257
- Wilson GWT, Rice CW, Rillig MC, Springer A, Hartnett DC (2009) Soil aggregation and carbon sequestration are tightly correlated with the abundance of arbuscular mycorrhizal fungi: results from long-term field experiments. *Ecol Lett* 12:452–461. <https://doi.org/10.1111/j.1461-0248.2009.01303.x>

# Electronic Supplementary material

## A) The adaptive dynamics method

In this part the symbol \* signal the ecological equilibrium and  $\hat{\alpha}$  the evolutionary one.

### The Canonical Equation

Adaptive dynamics rest on a series of hypotheses. This method models explicitly the evolutionary consequences on species density dynamics, and the feedback of species density on the evolutionary process (Dieckmann and Law 1996; Geritz et al. 1998). Evolution occurs via small mutation steps between which plant and pollinator densities reach the ecological equilibrium. Adaptive dynamics also assume clonal reproduction and a small phenotypic impact of the mutations. The differential equation describing the evolution of the phenotypic traits, known as the canonical equation (Dieckmann and Law 1996), is given by:

$$\frac{d\alpha}{dt} = \frac{1}{2} \mu \sigma^2 P^*(\alpha) \left. \frac{\partial \omega(\alpha_m, \alpha)}{\partial \alpha_m} \right|_{\alpha_m \rightarrow \alpha} \quad (\text{A1})$$

As explained in the main text the term  $\frac{1}{2} \mu \sigma^2 P^*(\alpha)$  corresponds to the phenotypic variability brought by the mutation process; with  $\mu$  the per individual mutation rate,  $\sigma^2$  the variance of the mutation phenotypic effect, and  $P^*(\alpha)$  the plant equilibrium density. The last term is the selective gradient and represents the effects of natural selection, via variations of the relative fitness of mutants  $\alpha_m$  given a resident population of attractiveness  $\alpha$ . Therefore, the sign of the selective gradient gives the direction of evolution; a positive gradient selects larger attractiveness, while a negative gradient selects smaller trait values. The relative fitness of a mutant at a very low density is explicitly derived from the ecological dynamics (equation (1) in main text). It is computed as the *per capita* growth rate of a rare mutant population in a resident population at ecological equilibrium :



$$\omega(\alpha_m, \alpha) = \frac{1}{P_m} \frac{dP_m}{dt} \Big|_{P_m \rightarrow 0} = r_P(\alpha_m) - c_P P^*(\alpha) + \alpha_m \gamma_A A^*(\alpha), \quad (\text{A2})$$

with  $P_m$  the mutant population density,  $P^*(\alpha)$  and  $A^*(\alpha)$  given by equation (3) in the main text.

Remember that, due to the allocation costs, the plant intrinsic growth rate varies with the level of attractiveness  $r_P(\alpha)$ .

## The singular strategies

Eco-evolutionary dynamics (equation A1) may exhibit equilibrium points, called evolutionary singular strategies. They correspond to trait values at which equation (A1) is at equilibrium, i.e., trait variation goes to zero.

Trait variations are given by the Canonical equation (A1). Because the first part of this equation is positive, the direction of trait variations is entirely determined by the selection gradient. When it is positive, higher trait values are selected, while negative selection gradients lead to smaller traits. Here the selection gradient corresponds to the slope of the fitness function A2 at the resident trait  $\alpha$ , given a small variation in the trait  $\alpha_m$ .

$$\frac{\partial \omega(\alpha_m, \alpha)}{\partial \alpha_m} = \frac{dr_P(\alpha_m)}{d\alpha_m} + \gamma_A A^*(\alpha), \quad (\text{A3})$$

Because of the hypothesis of small mutations, this yield:

$$\frac{\partial \omega(\alpha_m, \alpha)}{\partial \alpha_m} \Big|_{\alpha_m \rightarrow \alpha} = \frac{dr_P(\alpha_m)}{d\alpha_m} \Big|_{\alpha_m \rightarrow \alpha} + \gamma_A A^*(\alpha), \quad (\text{A4})$$

Because all other terms of the Canonical Equation (A1) are positive, the evolutionary singular strategy  $\hat{\alpha}$  correspond to trait values at which the selection gradient is null:

$$\frac{\partial \omega(\alpha_m, \alpha)}{\partial \alpha_m} \Big|_{\alpha_m, \alpha \rightarrow \hat{\alpha}} = \frac{dr_P(\alpha_m)}{d\alpha_m} \Big|_{\alpha_m, \alpha \rightarrow \hat{\alpha}} + \gamma_A A^*(\hat{\alpha}) = 0, \quad (\text{A5})$$

with  $r_P(\alpha)$  defined by equation (6) and  $A^*$  by equation (3) in the main article.

This means that a singularity is obtained only when costs in terms of energy of alternative means of reproduction  $\left(\frac{dr_P(\alpha_m)}{d\alpha_m}\right)_{\alpha_m, \alpha \rightarrow \hat{\alpha}}$  match the benefits in terms of pollination of increased attractiveness  $(\gamma_A A^*(\hat{\alpha}))$ .

Replacing  $r_P$ , we obtain:

$$\left.\frac{\partial \omega(\alpha_m, \alpha)}{\partial \alpha_m}\right|_{\alpha_m, \alpha \rightarrow \hat{\alpha}} = \frac{-\left(\frac{\hat{\alpha}}{\alpha_{max}}\right)^s \left(1 - \left(\frac{\hat{\alpha}}{\alpha_{max}}\right)^s\right)^{\frac{1}{s}-1}}{\hat{\alpha}} + \gamma_A \frac{\hat{\alpha} \gamma_P r_P(\hat{\alpha}) + c_P r_A}{c_A c_P - \hat{\alpha}^2 \gamma_A \gamma_P} = 0, \quad (A6)$$

In the linear case (i.e. when  $s = 1$ ), the singular strategy formula is:

$$\hat{\alpha} = \frac{c_P(c_A - \alpha_{max} \gamma_A r_A)}{\alpha_{max} \gamma_A \gamma_P} \quad (A7)$$

This solution is feasible (i.e. positive and in a plausible range value), with  $\alpha_{max} < \alpha_{cl}$  as defined in equation (4) of the main text, if and only if  $0 < c_A < \alpha_{max} \gamma_A r_A$ ; i.e. the intraspecific competitive losses need to stay below the maximal energetic gain of the animal.

In this linear case, increasing plant or animal losses or decreasing animal intrinsic growth rate (within the conditions for a feasible solution) will increase the singular strategy value, meaning that when these losses are high or the animal intrinsic growth low the plant invest more in the mutualistic interaction. On the contrary higher gains from the mutualistic interaction will lead into a lower investment in the plant attractiveness at eco-evolutionary equilibrium.

Aside from its existence, a singular strategy can be an endpoint of evolution if convergent (evolutionary dynamics locally lead to it) and non-invasible (it persists in time because of a resistance

to invasion by nearby mutants). The mathematical computation for the existence of singular strategies and their convergence and invasibility properties are given in the following part.

## B) Convergence and invasibility properties of the singular strategies

### The conditions for invasibility

With the trade-off function defined in main text equation (5) we can differentiate the fitness function a second time to analyse the convergence and invasibility of the singular strategies, to deduce the overall trait dynamics (Dieckmann and Law 1996). The singular strategy ( $\hat{\alpha}$ ) is non-invasible, i.e. an ESS (Maynard Smith, 1982) when:

$$\left. \frac{\partial \omega^2(\alpha_m, \alpha)}{(\partial \alpha_m)^2} \right|_{\alpha_m, \alpha \rightarrow \hat{\alpha}} = \frac{(1-s) \left( \frac{\hat{\alpha}}{\alpha_{max}} \right)^s \left( 1 - \left( \frac{\hat{\alpha}}{\alpha_{max}} \right)^s \right)^{\frac{1}{s}-2}}{\hat{\alpha}^2} < 0 \quad (\text{B8})$$

Concave trade-offs ( $s > 1$ ) therefore lead to non-invasible singular strategies, while convex trade-offs ( $s < 1$ ) yield invasible strategies.

In the case of a linear trade-off equation (B8) is equal to 0, the strategy is neutral from an invasibility point of view.

### The conditions for convergence

The previous equation, summed with the crossed derivation of the fitness function gives conditions for convergence of the singular strategy (Dieckmann and Law 1996). The singular strategy is convergent when:

$$\frac{\partial \omega^2(\alpha_m, \alpha)}{(\partial \alpha_m)^2} \Big|_{\alpha_m, \alpha \rightarrow \hat{\alpha}} + \frac{\partial \omega^2(\alpha_m, \alpha)}{\partial \alpha \partial \alpha_m} \Big|_{\alpha_m, \alpha \rightarrow \hat{\alpha}} < 0 \quad (\text{B9})$$

The above-mentioned formula requires the calculation of the cross-derivation. Using results from equation (A3), and with small mutation close to the singular strategy ( $\alpha_m, \alpha \rightarrow \hat{\alpha}$ ), it gives:

$$\frac{\partial \omega^2(\alpha_m, \alpha)}{\partial \alpha \partial \alpha_m} \Big|_{\alpha_m, \alpha \rightarrow \hat{\alpha}} = \gamma_A \frac{dA^*(\hat{\alpha})}{d\alpha} \quad (\text{B10})$$

According to the formula of  $A^*(\hat{\alpha})$  given in equation (3) of the main article, the previous equation is equivalent to:

$$\begin{aligned} \frac{\partial \omega^2(\alpha_m, \alpha)}{\partial \alpha \partial \alpha_m} \Big|_{\alpha_m, \alpha \rightarrow \hat{\alpha}} &= \frac{\gamma_A \gamma_P (2c_P \gamma_A r_A \hat{\alpha} + (c_A c_P + \hat{\alpha}^2 \gamma_A \gamma_P) r_P(\hat{\alpha}) + \hat{\alpha} (c_A c_P - \hat{\alpha}^2 \gamma_A \gamma_P) r_P'(\hat{\alpha}))}{(c_A c_P - \hat{\alpha}^2 \gamma_A \gamma_P)^2} \end{aligned} \quad (\text{B11})$$

with  $r_P(\hat{\alpha})$  defined by equation (6) in the main article, and  $r_P'(\hat{\alpha}) = r_P(\hat{\alpha}) \frac{1}{\hat{\alpha} \left(1 - \left(\frac{\hat{\alpha}}{\alpha_{max}}\right)\right)^{-s}}$ .

The sum of equation (B11) at the eco-evolutionary equilibrium (i.e. when  $\alpha_{max}, \alpha \rightarrow \hat{\alpha}$ ) and (B8) is however too complex in the general case to give a simple to understand the convergence condition (as required by equation B9)

In the linear case (i.e. when  $s = 1$ ), equation (B11) at the eco-evolutionary equilibrium becomes:

$$\frac{\partial \omega^2(\alpha_m, \alpha)}{\partial \alpha \partial \alpha_m} \Big|_{\alpha_m, \alpha \rightarrow \hat{\alpha}} = \frac{\gamma_A \gamma_P \left( c_A c_P + \hat{\alpha}^2 \gamma_A \gamma_P + 2c_P \hat{\alpha} \left( \gamma_A r_A - \frac{c_A}{\alpha_{max}} \right) \right)}{(c_A c_P - \hat{\alpha}^2 \gamma_A \gamma_P)^2} \quad (\text{B12})$$

Because then equation (B8)  $\left. \frac{\partial \omega^2(\alpha_m, \alpha)}{(\partial \alpha_m)^2} \right|_{\alpha_m, \alpha \rightarrow \hat{\alpha}} = 0$ , the convergence condition then depends only on the above cross derivation (B12).

According to equation (A7),  $\gamma_A r_A - \frac{c_A}{\alpha_{max}} = \frac{-\hat{\alpha} \gamma_A \gamma_P}{c_P}$ , equation (B12) when  $s=1$  is equal to:

$$\left. \frac{\partial \omega^2(\alpha_m, \alpha)}{\partial \alpha \partial \alpha_m} \right|_{\alpha_m, \alpha \rightarrow \hat{\alpha}} = \frac{\gamma_A \gamma_P}{(c_A c_P - \hat{\alpha} \gamma_A \gamma_P)^2} \left[ c_A c_P + \hat{\alpha}^2 \gamma_A \gamma_P - 2 c_P \hat{\alpha} \frac{\hat{\alpha} \gamma_A \gamma_P}{c_P} \right] \quad (B13)$$

Which, when simplifying gives:

$$\left. \frac{\partial \omega^2(\alpha_m, \alpha)}{\partial \alpha \partial \alpha_m} \right|_{\alpha_m, \alpha \rightarrow \hat{\alpha}} = \frac{\gamma_A^2 \gamma_P^2}{(c_A c_P - \hat{\alpha} \gamma_A \gamma_P)^2} - \left[ \frac{c_A c_P}{\gamma_A \gamma_P} - \hat{\alpha}^2 \right] \quad (B14)$$

Note that  $\frac{c_A c_P}{\gamma_A \gamma_P} = \alpha_{cl}^2$ . Because  $\hat{\alpha} < \alpha_{max} < \alpha_{cl}$ , when  $\hat{\alpha}$  exist, the above derivation is always positive, meaning that a linear trade-off always leads to a divergent singular strategy.

## C) Effect of the trade-off shape on the number of singular strategies

We prove in this section that  $s = 2$  (concave trade-off) is a threshold for the existence of a second singular strategy in the case  $r_A = 0$ .

For  $r_A = 0$  the singular strategies are the solution of the following equation (obtained by setting  $r_A = 0$  in equation (A6)):

$$\left. \frac{\partial \omega(\alpha_m, \alpha)}{\partial \alpha_m} \right|_{\alpha_m, \alpha \rightarrow \hat{\alpha}, r_A=0} = \frac{r_P (\hat{\alpha})^{(1-s)} \left( \hat{\alpha}^2 \gamma_A \gamma_P - \left( \frac{\hat{\alpha}}{\alpha_{max}} \right)^s c_A c_P \right)}{\hat{\alpha} (c_A c_P - \hat{\alpha}^2 \gamma_A \gamma_P)} = 0 \quad (C15)$$

If  $s > 1$ , then  $\hat{\alpha} = 0$  is always a solution. Now we can study the existence of a second non-zero singular strategy, which is then the solution of:

$$\hat{\alpha}^2 \gamma_A \gamma_P = \left( \frac{\hat{\alpha}}{\alpha_{max}} \right)^s c_A c_P \quad (C16)$$

The solution can be explored geometrically, but we first need to rewrite the equation as follow:

$$\hat{\alpha}^2 = \left( \frac{\hat{\alpha}}{\alpha_{max}} \right)^s \frac{c_A c_P}{\gamma_A \gamma_P} = \left( \frac{\hat{\alpha}}{\alpha_{max}} \right)^s \alpha_{cl}^2 \quad (C17)$$

Remember that the stability conditions impose that  $\frac{c_A c_P}{\gamma_A \gamma_P} = \alpha_{cl}^2 > \alpha_{max}^2$ . Now, we can plot the left and

the right side of equation (C17) as a function of  $\hat{\alpha}$  and the solution is given at the crossing of the two curves (figure C1). Note that only the right side depends on the value of the trade-off parameters.

Figure C1, shows that if  $1 < s \leq 2$  there exists a unique solution that is  $\hat{\alpha} = 0$ . This is because the right side is always larger than the left side for  $\hat{\alpha} > 0$ . Now, if  $s > 2$ , there exists a second solution, which is

$\hat{\alpha} = \sqrt[s-2]{\frac{\alpha_{cl}^2}{\alpha_{max}^s}}$ . This proof that at the value  $2 = s$  there is a branching from one to two singular

strategies. Now, the nature of the two strategies needs to be explored numerically, as well as how it extends to negative values of  $r_A < 0$ .

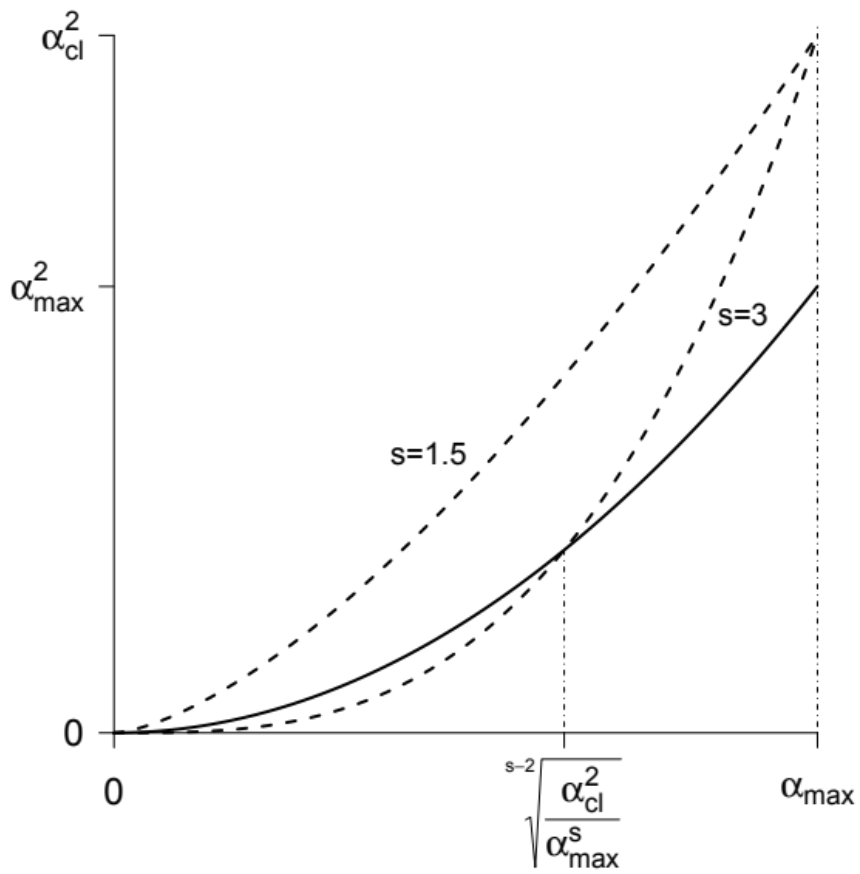


Figure C1: geometry

representation of equation (C17). The black line represents the left side of equation (C17), while the right side is given by the dashed line for two different values of the trade-off shape parameters  $s$ .

## D) Supplementary figures

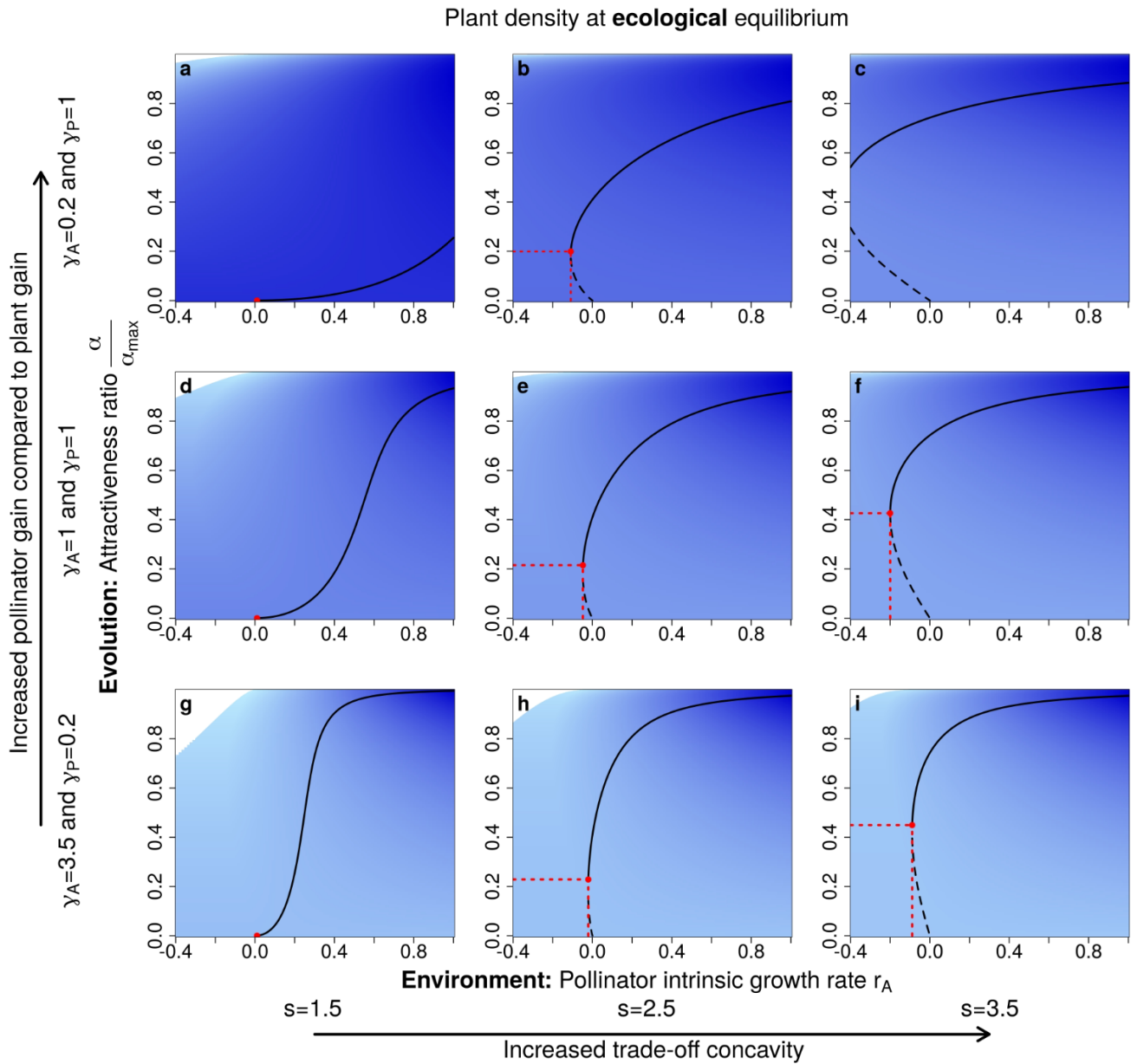


Figure D1: **Influence of trade-off shape and mutualistic gains on  $E^3$  diagrams.** As in figure 5 in the main text, columns differ in trade-off concavity. Lines differ in the asymmetry of mutualistic gains: in the top line (panels a, b, and c) pollinators benefit more than plants; the middle line (panels d, e, and f) shows equal gains while in the bottom line plant gains are larger. Red points and dotted lines represent the lowest  $r_A$  and  $\frac{\alpha}{\alpha_{max}}$  values for maintaining a CSS, allowing the maintenance of the mutualistic interaction. Colours and lines are the same as in figure 4 in the main text. The parameter values are  $c_A = c_P = 1$  and  $\alpha_{max} = 0.8 * \alpha_{cl}$ .

## E) References



Dieckmann U, Law R (1996) The dynamical theory of coevolution: a derivation from stochastic ecological processes. *J Math Biol* 34:579–612. <https://doi.org/10.1007/BF02409751>

Geritz S a. H, Kisdi E, Mesze NA G, Metz J a. J (1998) Evolutionarily singular strategies and the adaptive growth and branching of the evolutionary tree. *Evol Ecol* 12:35–57. <https://doi.org/10.1023/A:1006554906681>

Maynard Smith J (1982) *Evolution and the Theory of Games*. Cambridge University Press